

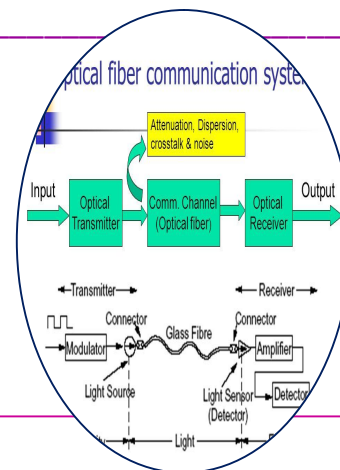


STUDIES ON FIBER DISPERSION FOR COMMUNICATION SYSTEM

Chandra Bhushan Kumar¹ And Dr. U.K.Das²

¹Research Scholar , L.N.M.U. Darbhanga .

²Dept. of Physics , C.M.Science College, Darbhanga .



ABSTRACT

We investigate theoretically and experimentally the detrimental effect of fiber dispersion on the synchronization of an optoelectronic phase chaos cryptosystem. We evaluate the root-mean square synchronization error and the cancellation spectra between the emitter and the receiver in order to characterize the quality of the optical fiber communication link.

KEYWORDS— Phase modulation, optical communications, & chaos cryptography,

INTRODUCTION

CHAOS communication systems require the use of transmitters and receivers operating in synchronized chaotic regime, even if located far one from another [1]. For optical fiber communication networks, the chaotic masking motion used for encryption is carried by a laser beam and this optical chaos can be generated using a wide variety of architectures (see refs. [2], [3] and references therein). In a recently proposed efficient and fast optical phase dynamics [4], [5], chaos is generated by combining electro-optical phase modulation, an external nonlinear phase-to-intensity converter, and a delay induced by an optoelectronic feedback loop (fiber, RF photodetectors, and amplifier).

As any communication system, chaos cryptosystems have to overcome the problem of signal-to-noise ratio at the receiver stage. In our case, this noise mainly arises from three different sources. The first source is constituted by the unavoidable stochastic fluctuations that are affecting the system; in order to minimize its influence, there is no other solution than to use optoelectronic components that are the less noisy possible. The second source is specific to chaos cryptosystems, and it is due to the various mismatches in parameters between the emitter and the receiver [6], [7], [8]. Theoretically, for an open loop self synchronizing scheme,

this noise vanishes when the emitter and the receiver are identical; but in practice, reducing this noise to a minimum requires a careful matching of the system components, or (in marginal cases) a fine tuning leading to a partial mismatch compensation [7]. The third source of noise will be the main purpose of this article; it arises from the encrypted signal distortion due to transmission over the communication channel. Effectively, the carrier is subjected to attenuation, Kerr nonlinearity and chromatic dispersion during its propagation in the fiber. In fact, the results reported here indicate a better synchronization performance when compared with previous measurements in electro-optical intensity chaos [9]. To the best of our knowledge, very few investigations have been devoted to the topic of fiber propagation effects on the performance of chaos cryptography [10], [11], [12], [13], and they were exclusively based on numerical simulations. Fiber transmission has been considered in some experimental works [3], [14], but no detailed analysis on the fiber dispersion effects has been reported. Our aim in this paper is to address this issue with a joint theoretical and experimental analysis.

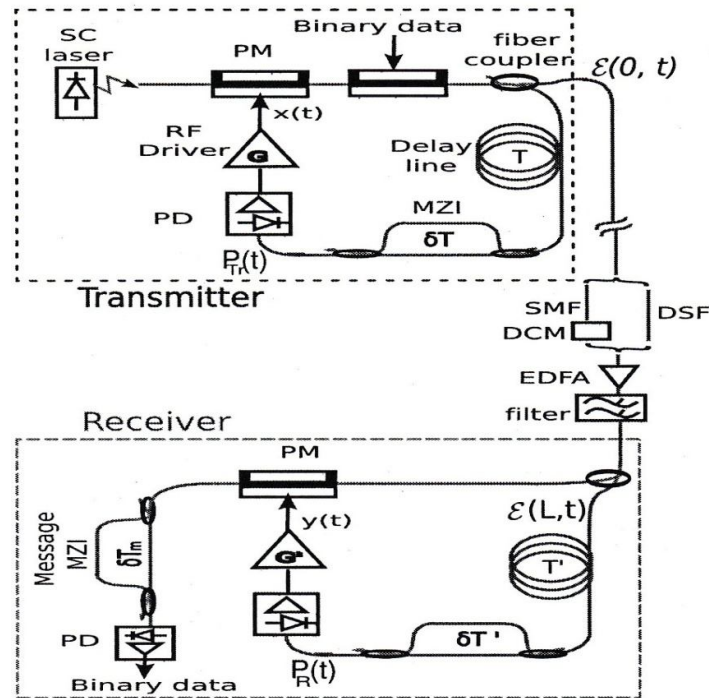


Fig. 1. Experimental setup. EDEA: erbium-doped fiber amplifier

THE SYSTEM

The schematic representation of the communication system under study is shown in Fig. 1. It is inspired by the work presented in ref. [4], [5], where the concept of nonlocal nonlinearity has been defined for chaos generation, as a consequence of the use of an imbalanced interferometer for performing nonlinear phase

to intensity demodulation. Three sub-systems can be distinguished: the transmitter, the channel, and the receiver. They are described in details in the next subsections.

Transmitter

The transmitter performs two operations: it encodes into the optical domain an original binary message through a classical differential phase shift keying electro-optic modulation. This optical phase modulation is subsequently hid-den within a broadband noise-like phase modulation, which is obtained through the principle of nonlocal nonlinear delay phase chaos generation.

The transmitter thus consists of a continuous-wave distributed feedback semiconductor laser feeding a LiNbO₃ phase modulator with the wavelength $\lambda = 2\pi c/\omega_0 = 1.55 \mu\text{m}$. This phase modulator having a halfwave voltage of V_π , receives the electrical chaotic input from a broadband radio-frequency (RF) driver, and translates this electrical signal modulation into the optical phase one while keeping the intensity unchanged. The optical phase therefore changes proportionally to the voltage applied to the modulator, and the time dependent phase shift introduced by the modulation is

$$\varphi(t) = \pi \cdot \frac{V(t)}{V_\pi} \quad (1)$$

The message is mixed with the chaos through a second cascaded phase modulator, which is assumed for simplicity to have the same V_π . The message phase modulation is performed by driving the modulator with a V_π peak-to-peak voltage in order to add a π phase shift, following the standard differential phase shift, so that the total optical phase at the output of the message phase modulator reads:

$$\frac{V(t)}{V_\pi} \quad \varphi(t) = \pi \cdot \frac{\pi(t)}{V_\pi} \quad (2)$$

Where $\pi(t) = \pm V_\pi$ is the message amplitude.

The electric field has only one vectorial polarization in our system, so that we can restrict ourselves to a scalar description of the optical field. The output is split into two parts, one is transmitted through the channel while the other enters in the delay line. The complex envelope of the electric field can be written as $\varepsilon(z, t)$, where z is the distance from the output of the message phase modulator, and t is time. For the transmitted part the dependence on z is taken into account in the next subsection dealing with fiber propagation. For the part going through the emitter loop we neglect any dependence on z since the effects of the fiber propagation within the transmitter are negligible. From Eq. (2), one has

$$\varepsilon(0, t) = E_0 \exp [i\psi(t)], \quad (3)$$

where $i^2 = -1$ and E_0 is the field amplitude. This envelope is then delayed by a time T while travelling through the optical feedback path in the transmitter.

The optical intensity at the MZI output is thus a non-linear nonlocal transformation of the phase modulation:

$$P_{Tr}(t) = P_0 \cos^2 \left\{ \frac{1}{2} [\omega_0 \delta T + \psi(t-T) - \psi(t-T-\delta T)] \right\}, \quad (4)$$

Where $P_0 = |E_0|^2 / (\mu_0 c)$, μ_0 being the vacuum permeability and c the speed of the light. This optical intensity is then converted to the electrical domain by a photodiode. This electrical signal is thus band-pass filtered by the electronics of the feedback loop, which RF frequency filtering process can be modelled in the time domain by an integro-differential operator characterized by a high and a low-frequency cut-off. For sake of simplicity we assume that the filter is linear and of second order, so that the dynamics of the input RF voltage at the input of the chaos phase modulator obeys

$$V(t) + T \frac{d}{dt} V(t) + \frac{1}{\theta} \int_{t_0}^t V(s) ds = \eta G_0 S P_{Tr}(t), \quad (5)$$

Where θ and T are the characteristic response times attached to the low and high cut-off frequencies of the filter respectively, G_0 stands for the amplifier gain, η accounts for overall optical losses, and S is the photodetection efficiency. Note that the condition $\tau \ll \theta$ has been taken into account in the above equation (easily fulfilled assumption, since the feedback filtering is broadband for telecom devices). For mathematical convenience we introduce the dimensionless variables $x(t)$ and $m(t)$ as follows:

$$\frac{V(t)}{2V_\pi} = \pi \frac{\phi(t)}{2}, \quad (6)$$

$$\frac{\mu(t)}{2V_\pi} = \pi, \quad (7)$$

so that Eq. (5) can be rewritten in the dimensionless form as

$$x(t) + \tau \frac{dx}{dt} + \frac{1}{\theta} \int_{t_0}^t x(s) ds = G \cos^2 \{x(t-T) - x(t-T-\delta T) + m(t-T) - m(t-T-\delta T) + \varphi_0\}, \quad (8)$$

Where $G = \pi\eta G_0 SP_0 / (2V_\pi)$ is the overall feedback loop gain, and $\varphi_0 = \omega_0 \delta T / 2$ is a constant offset phase. This equation rules the dynamics of the input RF voltage at the first phase modulator.

OPTICAL CHANNEL

According to the experimental setup shown in Fig. 1, the light beam launched into the fiber communication channel corresponds to the optical signal at the second phase modulator output. The transmitter modelling of Eq. (2) allows to derive the electric field envelope of that transmitted light as being expressed by:

$$E(0, t) = E_0 \exp \{2i[x(t) + m(t)]\}. \quad (9)$$

The propagation on the fiber can be described in the moving frame by [15]:

$$\frac{\partial \varepsilon}{\partial z} (z, t) = -\frac{\alpha}{2} \varepsilon(z, t) - i \frac{\beta_2}{dt} \frac{\partial^2 \varepsilon}{\partial t^2} (z, t) + i \frac{\beta_3}{6} \frac{\partial^3 \varepsilon}{\partial t^3} (z, t), \quad (10)$$

where β_2 is the second order dispersion, β_3 is the third order dispersion, γ is the nonlinear Kerr factor and α is the linear attenuation.

RECEIVER

The optical field arriving at the MZI is $\varepsilon(L, t - T_R)$, so the MZI intensity output is

$$P_R = \frac{1}{\mu c} \frac{1}{4} \left| \varepsilon(L, t - T') e^{i(2\varphi_0' + \pi)} + \varepsilon(L, t - T' - \delta T') \right|^2 \quad (11)$$

Where the prime (') indicates the receiver parameters. In order to remove the chaotic masking, the replicated chaos needs to have the opposite sign with respect to the emitter one. This is easily achieved experimentally operating

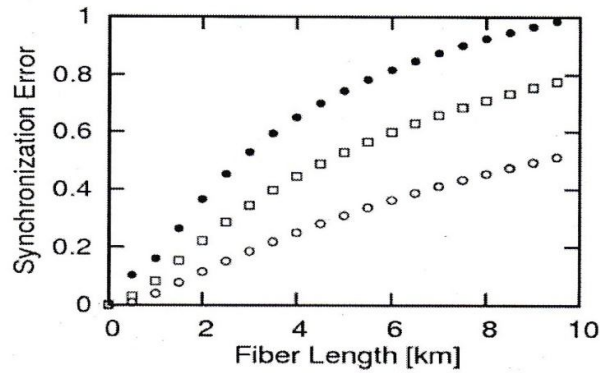


Fig. 2. Numerical simulation of the synchronization error between the emitter and receiver

The MZI with a π -shifted static phase as indicated in Eq. (11). Alternatively this could have been done using balanced photodiodes and exchanging their inputs or using an inverted amplifier at the receiver.

Under such conditions the normalized signal $y(t)$ driving the receiver phase modulator with an anti-replica of the chaotic masking, is ruled by the following “open loop” dynamics:

$$y(t) + \tau \frac{dy(t)}{dt} = \frac{1}{\theta'} \int_{t_0}^t y(s) ds = G' \frac{P_R(t)}{P_0} \quad (12)$$

where $G' = \pi \eta' G' S' / (2V'_{R\tau})$

The receiver electro-optic phase modulator applies an additional phase modulation onto the receiver light beam, proportionally to the signal $y(t)$. This leads to a total optical phase modulation proportional to $(x + y)$ at the chaos cancellation output. When a DPSK message modulation is applied at the transmitter, this sum is intended to retrieve the DPSK modulation only, the one proportional to $m(t)$, due to the anti-phase chaos replica expected for $y(t)$. The resulting light beam can then be processed through a standard DPSK demodulator matched with the message bit rate (imbalanced MZI with δT_m in Fig. 1). The photodiode detects

$$R(t) = \frac{1}{4S} \left| \varepsilon(L, t) e^{2iy(t)} + \varepsilon(L, t - \delta T_m) e^{2iy(t - \delta T_m)} \right|^2 \quad (13)$$

In the absence of a binary DPSK message, the sum $\varepsilon = (x + y)$ is used to evaluate the accuracy of the phase chaos cancellation. Similarly to the usual signal-to-noise ratio, a cancellation-to-chaos ratio can be defined in order to analyze the accuracy of the chaos cancellation in a normalized way.

NUMERICAL RESULTS: CANCELLATION NOISE

In this section, we theoretically investigate the time-domain variations of the cancellation noise when the fiber and the chaotic carrier parameters are varied. This analysis relies on the coupled Eqs. (8), (10) and (12) with the

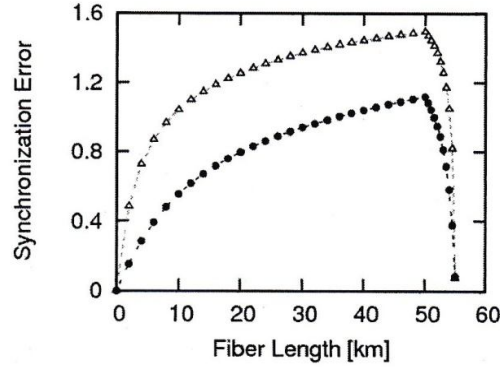


Fig. 3. Numerical simulation of the dispersion compensation using DCFs with $\beta_{2\text{DCF}} = -200 \text{ ps}^2/\text{km}$ $\beta_{3\text{DCF}} = 0.1 \text{ ps}^3/\text{km}$, $\alpha_{\text{DCF}} = 0.6 \text{ dB}$, $\gamma_{\text{DCF}} = 6 \text{ W}^{-1}$.

The values used for the feedback gains are $G = 2.5$ (●) and $G = 5.0$ (Δ). When the chaotic carrier is launched at $z = 0$, the synchronization error increases steadily but at $z = 50 \text{ km}$, a 5 km-long DCF is used and drastically reduces the cancellation noise. parameters $\tau = 20 \text{ ps}$, $\theta = 1.6 \text{ } \mu\text{s}$, $\delta T = 0.4 \text{ ns}$, $\varphi_0 = \frac{\pi}{4}$ and $T = 70 \text{ ns}$. The power P_0 is 5mW, and we consider a single mode fiber (SMF) for the transmission channel with parameters $\beta_2 = 20 \text{ ps}^2 \text{ km}^{-1}$, $\beta_3 = 0.1 \text{ ps}^2 \text{ km}^{-1}$, $\gamma = 1.1 \text{ W}^{-1} \text{ km}^{-1}$, $\alpha = 0.2 \text{ dB km}^{-1}$ (0.046 km^{-1}). we characterize the system performance using the normalized cancellation-to-chaos ratio defined as

$$\sigma = \sqrt{\frac{[\varepsilon^2(t)]}{[x^2(t)]}} \quad (14)$$

We remark that the perfect cancellation of the chaos is expected when $y(t)$ perfectly anti-synchronizes with $x(t)$.

Figure 2 illustrates clearly the dramatic influence of the fiber channel on the chaos cancellation at the receiver, when SMF only is involved in the optical link. The situation worsens as expected for higher feedback strength ($G = 5.0$), as this corresponds to an even broader chaotic spectrum to be conveyed through the dispersive channel (thereby it increases the linear frequency mixing effect of dispersion). For each situation reported in Fig. 2, we clearly see that a strong signal distortion occurs already for propagation over 10 km only of SMF. In this case, the message could not be successfully retrieved because the synchronization

error is too large. Typically, one would expect this error to be below 10%, which is of the order of the best experimental cancellation-to-chaos ratio due to residual parameter mismatch in a back-to-back configuration [4-17].

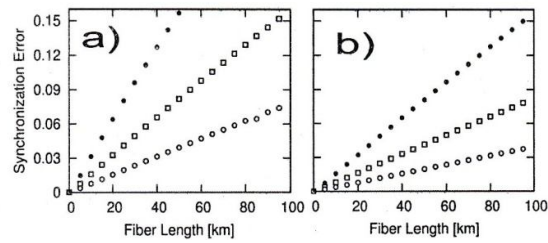


Fig. 4. Numerical simulation using DSFs. The values used for the gains are $G = 2.5$ (\circ), $G = 3.5$ (\square), and $G = 5.0$ (\bullet). (a) Synchronization error with the parameters $\beta_2 = 0.2 \text{ ps}^2\text{km}^{-1}$ and $\beta_3 = 0.1 \text{ ps}^3\text{km}^{-1}$.

Since the nonlinear effects are relatively weak in our context, the large distortion mainly originates from chromatic dispersion. This first result on a standard non compensated fiber channel shows that phase chaos communication is requiring necessarily a proper management of the dispersion effects.

CONCLUSION

we have shown that when propagating in standard SMFs, the broadband chaotic carriers are drastically affected by chromatic dispersion, and message recovery is impossible beyond few kilometres.

REFERENCES

- [1] K. M. Cuomo and A. V. Oppenheim, "Circuit implementation of synchronized chaos with applications to communications", Phys. Rev. Lett. Vol. 71, pp. 65-68, 1993.
- [2] S. Donati and C. R. Mirasso, Guest Editors, "Special issue on optical chaos and applications to cryptography", IEEE J. Quantum Electron., vol. 38, no. 9, Sept. 2002.
- [3] A. Argyris, D. Syvridis, L. Larger, V. Annovazzi-Lodi, P. Colet, I. Fischer, J. Garcia-Ojalvo, C. R. Mirasso, L. Pesquera and K. A. Shore, "Chaos-based communications at high bit rates using commercial fibre-optic links", Nature, vol. 438, pp. 343-346, 2005.
- [4] R. Lavrov, M. Peil, M. Jacquot, L. Larger, V. Udaltsov, and J. Dudley, "Electro-optic delay oscillator with nonlocal nonlinearity: optical phase dynamics, chaos and synchronization", Phys. Rev. E vol. 80, pp. 026207-1-9, 2009.
- [5] R. Lavrov, M. Jacquot, and L. Larger "Nonlocal nonlinear electro-optic phase dynamics demonstrating 10 Gb/s chaos communications" IEEE J. Quantum Electron., to appear 2010.
- [6] L. Larger, J-P. Goedgebuer, and F. Delorme, "Optical encryption system using hyperchaos generated by an optoelectronic wavelength oscillator", Phys. Rev. E, vol. 57, pp. 6618-6624, 1998.

- [7] Y. Chembo Kouomou, P. Colet, N. Gastaud, and L. Larger, "Effect of parameter mismatch on the synchronization of chaotic semiconductor lasers with electrooptical feedback", *Phys. Rev. E*, vol. 69, pp. 056226-1-15, 2004.
- [8] Y. Chembo Kouomou, P. Colet, L. Larger, and N. Gastaud, "Mismatch-induced bit error rate in optical chaos communication using semiconductor lasers with electrooptical feedback", *IEEE J. Quantum Electron.*, vol. 41, no. 2, pp. 156-163, 2005.
- [9] N. Gastaud, S. Poinot, L. Larger, J-M. Merolla, M. Hanna, J-P. Goedgebuer and F. Malassenet, "Electro-optical chaos for multi-10 Gbit/s optical transmissions", *Electron. Lett.*, vol. 40, pp. 898-899, 2004.
- [10] S. F. Yu, P. Shum, and N. Q. Ngo, "Performance of optical communication systems using multimode vertical cavity surface emitting lasers", *Opt. Commun.*, vol. 200, pp. 143-152, 2001.
- [11] A. Sanchez-Diaz, C. R. Mirasso, P. Colet, and P. Garcia-Fernandez, "Encoded Gbit/s digital communications with synchronized chaotic semiconductor lasers", *IEEE J. Quantum Electron.*, vol. 35, no. 3, pp. 292-297, 1999.
- [12] A. Bogris, D. Kanakidis, A. Argyris, and D. Syvridis, "Performance characterization of a closed-loop chaotic communication system including fiber transmission in dispersion shifted fibers", *IEEE J. Quantum Electron.*, vol. 40, no. 9, pp. 1326-1336, 2004.
- [13] D. Kanakidis, A. Bogris, A. Argyris, and D. Syvridis, "Numerical investigation of fiber transmission of a chaotic encrypted message using dispersion compensation schemes", *IEEE J. Lightwave Technol.*, vol. 22, no. 10, pp. 2256-2263, 2004.
- [14] A. Argyris, E. Grivas, M. Hamacher, A. Bogris, and D. Syvridis, "Chaos-on-a-chip secures data transmission in optical fiber links" *Optics Express*, vol. 18, pp. 5188-5198, 2010.
- [15] G. P. Agrawal, "Nonlinear fiber optics", 4th edition, Academic press, 2007.
- [16] Experimental spectra decay faster than numerical ones because the experimental filter is of higher order.
- [17] The decoded message $\mu\tau$ is to be compared with the input message going through an equivalent detection scheme involving a MZI with delay δT_m . Therefore Fig. 8 a) shows $\frac{1}{4}SP_0 \left| e^{im(t)} + e^{im(t-\delta T_m)} \right|^2$